Resonant pattern formation in active media driven by time-dependent flows

Vincente Pérez-Muñuzuri*

Group of Nonlinear Physics, Faculty of Physics, University of Santiago de Compostela. E-15782 Santiago de Compostela, Spain

(Received 20 September 2005; revised manuscript received 22 February 2006; published 12 June 2006)

The effect of a time-dependent flow in an oscillatory chemical system supporting front propagation is studied. Resonant target patterns depend on the strength and frequency of the time-dependent flow. The flow time scale needed to entrain the system to the resonant target period of oscillation depends on the closeness to the natural oscillation frequency of the medium. The flow strength needed to obtain these patterns is interpreted in terms of mixing optimization, and we give conditions for the flow that guarantee the best mixing with the Bernoulli property.

DOI: 10.1103/PhysRevE.73.066213 PACS number(s): 82.40.Ck, 47.54.−r, 47.70.Fw, 83.50.Xa

Spatiotemporal pattern formation has attracted the attention of researchers since long ago. However, the combined effects of reaction, diffusion, and advection have recently become an area of active research. This occurs especially in chemical reactions in a fluid environment [1], combustion systems in the presence of chaotic stirring by a laminar flow [2], dynamics of oceanic plankton populations [3], conversion of pollutants in the atmosphere [4], the depletion of the ozone layer [5], chaotic mixing in excitable media [6], or mixing of non-Newtonian fluids [7], to cite only some examples of the wide variety of industrial, theoretical, and environmental problems where reaction-advection-diffusion systems are relevant.

To date, many theoretical [8] and experimental [9] works have been written describing the effects of stirring in oscillatory chemical reactions. These effects manifest themselves as changes in the oscillatory period and amplitude, and even in the cessation or reappearance of oscillations. However, in spatiotemporal oscillatory media, the effects of mixing have not been investigated in detail [10]. The time scale of diffusive transport on macroscopic length scales is typically much longer than the characteristic time scale of the oscillations. A reaction-diffusion system forced by a time-dependent flow entrains to the forcing for certain values of the perturbation frequency and strength of the flow, then favoring resonant conditions that could not be achieved in classical reaction-diffusion problems. Although the entrainment phenomena are observed in a wide range of biological, chemical, and physical systems [11], as far as we know, this behavior has not been observed in reaction-advection-diffusion systems. It is often assumed that increasing stirring leads to spatial homogenization, but we will show that for time-dependent flows this resonant condition leads to regular pattern formation, even when mixing is increased.

The aim of this paper is to study the spatiotemporal pattern formation in a system driven by a nonlinear chemical dynamics corresponding to an oscillatory chemical reaction coupled with diffusion and advection. The advective flow used in this paper corresponds to two alternatively rotating point vortices, also called *blinking vortex flow* [12]. For specific values of the blinking period and the distance between vortices, the medium is entrained to the forcing and a coherent resonant regular structure (target patterns [13]) develops. We will show, both numerically and theoretically, the existence of a minimum distance between the blinking vortices in order to obtain a regular pattern. For that purpose, we will use a mathematical result on mixing in flows that could be represented in terms of *linked twist maps* that have the Bernoulli property [14,15].

The model used in this paper is

$$\frac{\partial \mathbf{C}}{\partial t} + (\mathbf{V}\cdot\boldsymbol{\nabla})\mathbf{C} = \mathbf{F}(\mathbf{C}) + D\nabla^2\mathbf{C}. \quad (1)$$

Here $\mathbf{C}=[C_u, C_v]$, $\mathbf{F}=[1-(B+1)C_u+AC_u^2C_v, BC_u-AC_u^2C_v]$ ($A,B>0$, Brusselator kinetics) [16] and the diffusion matrix is diagonal with coefficients (D_u,D_v). The velocity flow $\mathbf{V}$ consists of two corotating point vortices separated by a fixed distance $2b$ ($0<b<N/2$, N size of the medium), that blink on and off periodically with a constant period T. The velocity field is assumed to be independent of the concentration vector $\mathbf{C}$. This flow can be described by the following set of equations in Cartesian coordinates:

$$V_x = -\frac{\Gamma y}{x_s^2+y^2}, \quad V_y = \frac{\Gamma x_s}{x_s^2+y^2}, \quad (2)$$

where Γ is the flow circulation and

$$x_s = \begin{cases} x+b, & 0<t<T/2 \\ x-b, & T/2<t<T \end{cases}. \quad (3)$$

The blinking period T can be characterized by the nondimensional number $\mu=\Gamma T/b^2$. Increasing the flow strength μ leads to a chaotic flow above some critical value μ_c [14]. Another important feature to explain the results below is that independently of the μ value, the flow remains bounded (i.e., chemical species are not attracted into the flow from larger distances). Besides, mixing efficiency increases with μ for the range of values used here [14].

The reaction-advection-diffusion problem was integrated on a $N\times N$ square lattice using an implicit method for advection and diffusion (spatial step size $\Delta=1$) with a fourth-order Runge-Kutta with time step $\Delta t=0.001$ for the time integration of the local chemical dynamics. Zero flux boundary con-

*Electronic address: vicente.perez@cesga.es

 ©2006 The American Physical Society

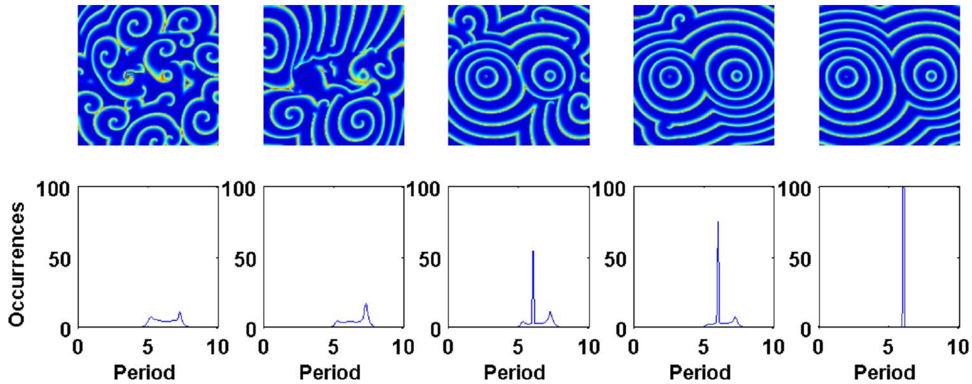

FIG. 1. (Color online) Sequence of C_u spatial fields (upper row) and their corresponding wave period histograms (lower row) for different values of the distance between vortices b in the blinking flow. Note the formation of two target waves that progressively fill the medium as b is increased. Mean wave periods (units of time) were calculated at each grid point and their distribution shown in terms of a histogram. From left to right; $b=22$, $b=34$, $b=36$, $b=38$, and $b=48$, respectively. The value of $b_{\mathrm{min}}=42$ was obtained by a numerical procedure that detects single-valued peaks. Set of parameters: $A=1$, $B=3$, $D_u=0.5$, $D_v=0$, $N=160$, $\Gamma=24$, and $T=6$ t.u.

ditions are imposed for the concentration gradients. Random initial conditions are set for the concentration field, and the flow is switched on at $t=0$. In the absence of advection, the resulting pattern is an ensemble of spiral waves interacting among them, with a natural wave period $T_{\mathrm{spiral}} \approx 6$ t.u. (where t.u. denotes time units). The model (1)–(3) is investigated for different flow strengths μ, by varying independently either b, T, or Γ. The influence of the diffusion on the obtained results is also studied.

The effect of the blinking vortex flow on the chemically oscillatory medium described by the Brusselator kinetics is shown in the upper sequence of pictures in Fig. 1. As the vortex distance b increases (keeping constant T and Γ), the resulting pattern moves from an ensemble of interacting spiral waves (equivalent to those obtained without advection) to a coherent structure consisting of two targets centered on the vortices position whose period of wave emission is equal to the blinking period T. Waves are emitted alternatively from the left and right positions with a time delay equal to $T/2$. These coherent-regular structures remain unchanged for larger values of b above some minimum value b_{min}. For smaller values of b, targets compete with spiral waves.

The lower sequence of images in Fig. 1 summarizes in terms of period histograms the results shown in the upper panels. At low values of b, the period histogram is wide, indicating poor correlation between separate regions in the system. This histogram does not change appreciably until reaching the minimum distance between vortices needed to get the target regular pattern, b_{min}. Near the threshold, the histogram shows that most points in the domain oscillate with the same frequency (corresponding to the target wave emission), although some peaks to the left and right of the main peak indicate that target patterns have not yet dominated all of the medium, as some spiral waves still survive and compete with them for free space. After the threshold, both targets are the only patterns in the domain with a wave period equal to the blinking period T.

Figure 2 shows the evolution of the mean wavelength as the vortices distance b is increased. The transition to a regular target wave pattern is smooth, changing from an approximate constant value corresponding to the case without target waves in the medium, but with multiple rotating spiral waves, to a higher constant wavelength after the threshold is crossed ($b \geqslant b_{\mathrm{min}}$).

The effect of the remainder parameters in order to obtain a regular structure with wave period T is analyzed in Fig. 3 for two values of the diffusion coefficient D_u and two domain sizes N. Data points in the figure correspond to values of Γ for which there exists a minimum value of b, b_{min}; above it, regular target patterns can be obtained. For lower values of Γ, outside of this range, the active medium is not disturbed by the advective flow, spiral waves are the dominant patterns, and no value of b leads to target pattern formation. On the other hand, for larger values of Γ than those shown in both graphs in Fig. 3, b_{min} remains constant and, for $b < b_{\mathrm{min}}$, wave fronts are broken by successive stretching and folding due to the hydrodynamics giving rise to free ends and then to spiral waves.

In order to obtain a coherent regular structure, for intermediate values of the vortex circulation Γ, smaller values of the vortices distance are needed. Following the curve $b_{\mathrm{min}}(\Gamma)$ until reaching its minimum value, the flow strength μ increases; thus, the area of the medium that is affected by both vortices (i.e., chemical species can be attracted toward the vortices in that area), also increases. Vortices do not need to

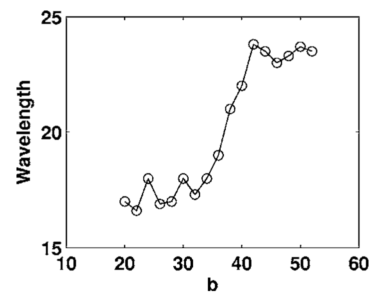

FIG. 2. Mean wavelength as a function of the distance between vortices b. Wavelengths are measured directly from the spatial C_u field with Fourier transform, and finally, a time average is done. Parameters as in Fig. 1.

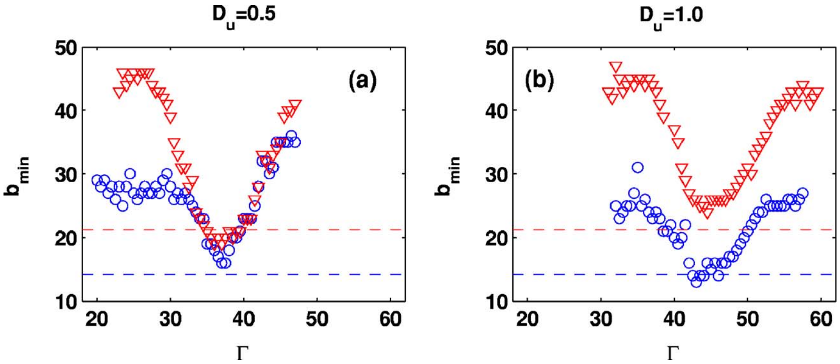

FIG. 3. (Color online) Minimum distance between vortices $b_{\min}$ as a function of the vortex circulation Γ for two different values of the diffusion coefficient D_u. Dashed lines follow from Eq. (7). Triangles and circles correspond to $N=120$ and $N=80$, respectively. Rest of parameters as in Fig. 1.

be as separated as for lower values of Γ in order to obtain the target patterns. Note that for $b < b_{\min}$, for any Γ, targets originated at the vortices centers cannot develop completely and interact with existing spiral waves. $b^c_{\min}$ is the minimum $b_{\min}$ value in both graphs in Fig. 3 that changes with the size of the domain and the diffusion. $b^c_{\min}$ is attained for larger values of Γ as D_u is increased. Spiral waves drift outside the domain, pushed by the higher-frequency target waves, faster with decreasing diffusion [17]. Then, it is expected that larger flow circulations should be needed in order to get only target waves in the medium when diffusion is increased. In other words, by increasing the flow strength (mixing efficiency), larger vortex circulations are needed to obtain only target waves with the highest frequency of the medium.

For a range of blinking periods $T \pm \omega \cong 6 \pm 0.6$ t.u., close to the natural period T_{spiral} the active medium is able to match its frequency to the periodic flow. Blinking periods outside of this range were not able to entrain the system to the forcing, and target patterns were not obtained for any value of b or Γ. Larger values of B in the Brusselator model require different ranges of blinking periods, and similar qualitative results were obtained (not shown here).

The existence of $b^c_{\min}$ can be related to the optimization of mixing in a two-dimensional (2D) flow described by Wiggins and Ottino [15]. Their argument stresses the necessary and sufficient conditions that lead to the best mixing. The key point was to define a 2D bounded time-dependent flow in a domain with solid boundaries and two transversally intersecting annuli in each half cycle. Their annuli, with inner and outer radii, r_i and r_o, respectively, should verify that

$$r_i - b > 0, \quad r_i + 2b > r_o \tag{4}$$

to ensure that the inner and outer circles of both annuli (centered on the positions of both vortices) intersect transversely. Besides, Wiggins and Ottino force the outer circles of the annuli to not protude outside of the domain,

$$b + r_o < \frac{N}{2}. \tag{5}$$

Nevertheless, this condition does not allow the corners of the medium to be well mixed, as mixing is Bernoulli defined only on the union of the two annuli ($A_1 \cup A_2$). For the best case, only a fraction of the domain (78%) is well mixed [15]. In our case, vortices should be able to influence the whole domain, including the corners, to guarantee the target patterns originated at the vortices position to spread along the domain, i.e., mixing should occur all along the domain area. Then, we relax the last condition (5) as

$$r_o^2 \geqslant \frac{N^2}{4} + b^2, \tag{6}$$

i.e., the outer circles intersect outside the domain, far enough to guarantee the union of both annuli to cover the whole domain ($A_1 \cup A_2 \geqslant N^2$). Thus, following Wiggins and Ottino [15], we obtain the minimum distance between vortices that ensure all the domain to be well mixed

$$\frac{b}{N} \geqslant \frac{1}{2\sqrt{8}}. \tag{7}$$

The mathematical results presented here apply to a given pair of annuli, one in each half cycle of the advection cycle, on which the hypotheses above are satisfied. The dashed line in Fig. 4 corresponds to the minimum b value of Eq. (7) for different N, while the dotted-dashed line corresponds to the optimal region of mixing $b \geqslant N/8$ obtained by Wiggins and Ottino [15]. Data points were obtained by fitting the numerical data in Fig. 3 to a Gaussian curve for different diffusion coefficients and medium sizes. For small medium sizes, the match between theory and numerical data is within the fitting error, while for large media, $b^c_{\min}$ is smaller than the theoretically predicted value (7), but still larger than Wiggins and Ottino's value.

We expect our results to be characteristic for a broad range of time-dependent chemical flows with oscillatory ki-

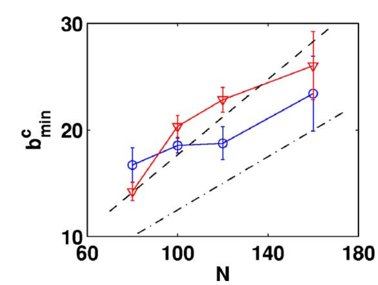

FIG. 4. (Color online) $b^c_{\min}$ as a function of the lattice size N. Triangles and circles correspond to $D_u=1.0$ and $D_u=0.5$, respectively. Dashed line follows from Eq. (7) and dotted-dashed line corresponds to the optimal region of mixing $b \geqslant N/8$ obtained by Wiggins and Ottino [15]. Rest of parameters as in Fig. 1.

netics. Time-dependent flows are a necessary condition for chaotic advection, and this is known to enlarge mixing in unsteady laminar flows [14]. However, boundary conditions and the time scale introduced by the flow (similar to the natural period of oscillation of the active media) have been shown to be responsible for the formation of target waves. Like entrainment phenomena in nonlinear oscillators, for an adequate set of parameters of the flow, increasing the mixing efficiency can lead to regular periodic pattern formation. In this sense, a single vortex ($T \rightarrow \infty$) could not force the system to target wave formation as the necessary condition of periodicity is not fulfilled. Hopefully, this entrainment phenomenon, observed experimentally in reaction-advection-diffusion systems, could be used for controlling the dynamics of oscillatory systems under stirring.

ACKNOWLEDGMENTS

We thank E. Hernández-García and V. Pérez-Villar for useful comments and a careful reading of the manuscript. This work was supported by Ministerio de Educación y Ciencia under Research Grant No. FIS2004–03006.

[1] C. R. Nugent, W. M. Quarles, and T. H. Solomon, Phys. Rev. Lett. **93**, 218301 (2004).

[2] I. Z. Kiss, J. H. Merkin, S. K. Scott, P. L. Simon, S. Kalliadasis, and Z. Neufeld, Physica D **176**, 67 (2003); I. Z. Kiss, J. H. Merkin, and Z. Neufeld, *ibid.* **183**, 175 (2003).

[3] E. R. Abraham, Nature (London) **391**, 577 (1998); E. R. Abraham *et al.*, *ibid.* **407**, 727 (2000).

[4] A. Wonhas and J. C. Vassilicos, Phys. Rev. E **65**, 051111 (2002); D. Poppe and H. Lustfeld, J. Geophys. Res. **101**, 14373 (1996).

[5] S. Edouard *et al.*, Nature (London) **384**, 444 (1996); O. Paireau and P. Tabeling, Phys. Rev. E **56**, 2287 (1997).

[6] Z. Neufeld, Phys. Rev. Lett. **87**, 108301 (2001); C. Zhou, J. Kurths, Z. Neufeld, and I. Z. Kiss, *ibid.* **91**, 150601 (2003).

[7] P. D. Anderson, O. S. Galaktionov, G. W. M. Peters, F. N. van de Vosse, and H. E. H. Meijer, J. Non-Newtonian Fluid Mech. **93**, 265 (2000).

[8] J. A. Aronovitz and D. R. Nelson, Phys. Rev. A **29**, 2012 (1984); J. Boissonade and P. DeKepper, J. Chem. Phys. **87**, 210 (1987); P. Ruoff, J. Phys. Chem. **97**, 6405 (1993).

[9] I. Nagypal and I. R. Epstein, J. Chem. Phys. **89**, 6925 (1988); L. López-Tomás and F. Sagués, J. Phys. Chem. **95**, 701 (1991); F. Ali and M. Menzinger, *ibid.* **96**, 1511 (1992); V. K. Vanag and D. P. Melikhov, *ibid.* **99**, 17372 (1995).

[10] Z. Neufeld, I. Z. Kiss, C. Zhou, and J. Kurths, Phys. Rev. Lett. **91**, 084101 (2003); I. Z. Kiss, J. H. Merkin, and Z. Neufeld, Phys. Rev. E **70**, 026216 (2004).

[11] M. H. Jensen, P. Bak, and T. Bohr, Phys. Rev. Lett. **50**, 1637 (1983); G. B. Ermentrout, J. Math. Biol. **29**, 571 (1991); L. Glass and J. Sun, Phys. Rev. E **50**, 5077 (1994); M. Braune and H. Engel, Chem. Phys. Lett. **211**, 534 (1993); O. Steinbock, V. Zykov, and S. C. Müller, Nature (London) **366**, 322 (1993); A. L. Lin, A. Hagberg, E. Meron, and H. L. Swinney, Phys. Rev. E **69**, 066217 (2004).

[12] H. Aref, J. Fluid Mech. **143**, 1 (1984); D. V. Khakar, H. Rising, and J. M. Ottino, *ibid.* **172**, 419 (1986).

[13] A. E. Bugrim, M. Dolnik, A. M. Zhabotinsky, and I. R. Epstein, J. Phys. Chem. **100**, 19017 (1996); H. Zhang, B. Hu, and G. Hu, Phys. Rev. E **68**, 026134 (2003); Y. Q. Fu, H. Zhang, Z. Cao, B. Zheng, and G. Hu, *ibid.* **72**, 046206 (2005).

[14] J. M. Ottino, *The Kinematics of Mixing* (Cambridge University Press, Cambridge, England, 1989).

[15] S. Wiggins and J. M. Ottino, Philos. Trans. R. Soc. London, Ser. A **362**, 937 (2004).

[16] For $B_c = 1 + A$, a Hopf bifurcation occurs and in the vicinity of the bifurcation point the period of the limit cycle is $T_{osc} \approx 2\pi/\sqrt{A}$.

[17] Spiral wave drift velocity increases with decreasing diffusion ($V_{drift} \propto 1/\sqrt{1+\alpha D^2}$, $\alpha > 0$). See also, A.S. Mikhailov, *Foundations of Synergetics I* (Springer-Verlag, Berlin, 1990).